

A primer on treatment planning aspects for temporally modulated pulsed radiation therapy

Christian Velten^{a,b}, Jiayi Huang^c, Wolfgang A. Tomé^{a,b,*}

^a*Montefiore Medical Center, Department of Radiation Oncology, Bronx, NY, USA*

^b*Albert Einstein College of Medicine, Institute for Onco-Physics, Bronx, NY, USA*

^c*Washington University, School of Medicine, Department of Radiation Oncology, Saint Louis, MO, USA*

Abstract

Temporally modulated pulsed radiotherapy (TMPRT) delivers conventional fraction doses of radiation using temporally separated pulses of low doses (<30 cGy) yielding fraction-effective dose rates of around 6.7 cGy min^{-1} with the goal to exploit tumor radiation hypersensitivity, which was observed in both, preclinical models and in human clinical trials. To facilitate TMPRT, volumetric modulated arc therapy (VMAT) and 3D-CRT planning techniques were developed following the guidelines of the proposed NRG CC-017 trial. Plans were evaluated with respect to HI, conformality, and adherence to dose constraints. Deliverability of plans was assessed using in-phantom measurements for absorbed dose accuracy at low dose rates and using EPID for isodose verification. For VMAT only single arc plans were found to be acceptable due to otherwise unacceptably heterogeneous field doses, while for dynamic conformal arc machine limitations on the number of monitor units per degree require the use of partial arcs for each pulse. Delivery of plans at low dose rates ($\leq 100 \text{ MU/min}$) was accurate with high Γ pass rates on modern LINACs and moderate pass rates on legacy LINACs, in line with their general performance. Generally, VMAT is preferred to achieve optimal homogeneity, conformality, and OAR sparing, while the use of 3D-CRT can increase the availability of TMPRT for more patients and clinics.

Keywords: temporally modulated, pulsed radiotherapy, radiation hypersensitivity, treatment planning, NRG CC-017

1. Introduction

Over the past decades, radiobiologists and radiation oncologists alike have observed that certain tumors are particularly sensitive to radiotherapy (RT) delivered

with low-dose rates of $<1.67 \text{ cGy min}^{-1}$,^{1,2} which supported the use of low-dose rate brachytherapy. This effect was also demonstrated in preclinical human glioblastoma (GBM) models where increased G2/M arrest was observed with continuous dose rates of $0.67 \text{ cGy min}^{-1}$.^{3,4} Additionally, investigators at the Gray Laboratory demonstrated that most tumor cells, including

*Corresponding author

Email address: wtome@montefiore.org
(Wolfgang A. Tomé)

GBM, exhibit hyper-sensitivity to low radiation doses <30 cGy due to a lack of ATM pathway activation for DNA repair.^{5–8} These two effects combined have given rise to a RT technique often referred to as pulsed low-dose rate, pulsed reduced-dose rate, or temporally modulated pulsed radiotherapy (TMPRT), where a conventional fraction dose of 180 cGy to 300 cGy is delivered in pulses of approximately 20 cGy, below the hyper-sensitivity threshold of around 30 cGy and with pulses sufficiently separated in time to yield low effective-dose rates of approximately 6.67 cGy min⁻¹.⁹ Since the instantaneous dose rate of RT delivery is not changed but rather temporally modulated, TMPRT may be the more accurate and preferred name for this technique. The efficacy of this approach has been demonstrated in preclinical tumor models, including GBM.^{10–12}

In addition to preclinical investigation, TMPRT has been successfully used at multiple institutions for reirradiating recurrent cranial and extra-cranial tumors.^{13–22} A prospective, single-arm phase II study has shown promising clinical efficacy of the combination of TMPRT and temozolomide (TMZ) on survival, neurocognitive function, and quality of life in adult patients with newly diagnosed GBM.²³ Another prospective, single-arm phase II study also evaluated TMPRT and TMZ in adult patients with newly diagnosed GBM and recently completed accrual ([NCT04747145](#)). There are two other prospective single-arm phase II studies examining TMPRT with or without concurrent bevacizumab for reirradiating recurrent high-grade glioma ([NCT01743950](#)) or IDH-mutant glioma ([NCT05393258](#)). A recently published evidence-based practice guideline by the American Society for Radiation Oncology

(ASTRO) endorsed TMPRT as an appropriate RT technique for irradiating or reirradiating GBM.²⁴

This work is intended as a primer on the treatment planning aspects for TMPRT to facilitate its use, specifically as part of the proposed NRG CC-017 trial, a randomized phase III study that compares TMPRT to standard RT in adult patients with newly diagnosed MGMT-unmethylated GBM. 3D-conformal radiotherapy (3D-CRT) and intensity-modulated planning techniques were evaluated and described as recipes, complete with plan evaluation metrics and measurement-based deliverability verification of these low-dose and low-dose rate pulses on various linear accelerators (LINACs).

2. Methods

Throughout this manuscript absorbed radiation doses are given in centigray (1 cGy equal to 0.01 Gy) in keeping with NRG conventions and for consistency with the proposed NRG CC-017 trial.

In TMPRT the fraction dose D_{fx} is delivered in discrete radiation pulses separated in time, resulting in a low fraction-effective dose rate,

$$\langle \dot{D} \rangle_{fx} = \frac{D_{fx}}{t_{b,1} - t_{b,n} + \Delta t},$$

with the beginning of first and last pulses, $t_{b,1}$ and $t_{b,n}$, and the nominal time between pulses, Δt . For example, a dose of 200 cGy delivered in ten pulses, with each pulse start separated by Δt of 3 min results in a dose rate of 6.7 cGy min⁻¹. This formula can also be used to calculate the minimum treatment session time required for each TMPRT fraction, which is approximately 30 min in the example above, excluding patient setup

and necessary imaging. For completeness, one can also consider the immediate effective dose rate which is the Δt -moving average over the delivered dose rate and which should similarly be below the low-dose rate threshold,

$$\langle \dot{D} \rangle(t) = \frac{1}{\Delta t} \int_{t-\Delta t}^t \dot{D}(t') dt'.$$

2.1. Planning techniques

Planning technique for TMPRT were developed as recipes using the Varian Eclipse treatment planning system (TPS) for 3D-CRT (simple & dynamic conformal arc (DCA)) and volumetric modulated arc therapy (VMAT) such that delivery of one field corresponds to one pulse. Deliverability and dose homogeneity over the delivered field in each pulse were primary goals in addition to the evaluation metrics described next.

2.2. Evaluation metrics

VMAT plans were generated according to the planning techniques for three unique LINACs: a Varian Trilogy with Millennium-120 multi leaf collimator (MLC), TrueBeam Edge with HD-120 MLC, and Halcyon with its layered SX2 MLC. For 3D-CRT plans were only generated for the TrueBeam Edge as no difference in machine performance is expected for this technique. Plans were evaluated using target coverage, homogeneity, and conformity metrics in addition to any applicable organ at risk (OAR) constraints. Here, the target homogeneity index (HI) is following the definition in ICRU 83,²⁵

$$HI = \frac{D_{2\%} - D_{98\%}}{D_{50\%}}, \quad (1)$$

while conformity is assessed using the Padnick conformality index and its two components, the *modified PITV ratio* (CI_{TV}) and the *overtreatment ratio* (CI_{PIV}):²⁶

$$CI_{\text{Padnick}} = \underbrace{\frac{TV \cap PIV}{TV}}_{CI_{TV}} \cdot \underbrace{\frac{TV \cap PIV}{PIV}}_{CI_{PIV}}. \quad (2)$$

The metrics and criteria used here and proposed for the clinical implementation of TMPRT are summarized in Table 1. Target and OAR constraints closely follow the proposed NRG-CC017 trial with absolute dose constraints given in the appendix (Tab. 5).

Table 1: Suggested target metrics and criteria for implementation of TMPRT. Percentages were calculated to closely follow the NRG-CC017 trial.

Metric	Constraint	Acceptable Variation
$D_{95\%}$	$\geq 98.75\%$	$\geq 95\%$
$D_{10\%}$	$\leq 105\%$	$\leq 108.3\%$
$D_{0.03 \text{ cm}^3}$	$\leq 106.7\%$	$\leq 110\%$

2.3. Plan delivery measurements

Absolute dose verification was performed by performing in-phantom ionization chamber measurements using a PTW N31010 on a Varian TrueBeam Edge. A charge-to-dose conversion factor was calculated by using a $10 \times 10 \text{ cm}^2$ reference field irradiation with 100 MU, which also corrects for daily output variations. The absorbed dose was measured at least five times for each distinct pulse. Measurement-based isodose verifications were performed for VMAT using electronic portal imaging device (EPID) on three linear accelerators: Varian Trilogy, TrueBeam Edge, and Halcyon. Measurements on the Trilogy unit were performed for portal dosimetry plans generated with

100 MU/min and 600 MU/min as set dose rates.

3. Results

3.1. Planning recipes

The following recipes were developed for both fractionation regimen in NRG-CC017, 4600 cGy to 6000 cGy in 200 cGy fractions (conventional) and 4000 cGy in 15 fractions (hypofractionation). For any other regimen one may follow the same overall approach. Field dose rates should be set to the larger of 100 MU/min or the lowest available for the machine. Field normalization for dose calculation should be set to 100 % at isocenter when available in the TPS.

3.1.1. VMAT with single arc

Enable TPS features to increase convergence requirements to improve plan quality for this single arc configuration (e.g., for Eclipse set *convergence mode*: "*Extended*" and *restart from MR level*: *MR3*). While the collimator rotation may be chosen freely, alignment more perpendicular to the arc plane will allow for improved modulation, especially for targets with OAR overlap in the inferior direction.

For conventional fractionation, create a plan with 20 cGy/fx and 230 fractions (70 for boost) for a total dose of 4600 cGy (1400 cGy) using a single full arc with a control point spacing not exceeding 2° (or whichever the minimum is for the TPS and treatment machine). Optimization of the plan may be done as usual with the exception that the number of arcs must stay fixed at one. After plan normalization the single arc is copied for a total of ten arcs with the arc direction reversed on alternating arcs (Tab. S1). Subsequently, the plan is recalculated with fixed monitor units (MUs)

for a prescription of 200 cGy/fx and 23 fractions (7 for boost). Each arc within the 200 cGy/fx plan is then delivering one pulse of 20 cGy. The resulting dose distribution for an example single arc VMAT plan is shown in the left column of Figure 1.

For hypofractionation, create a plan with 20.5 cGy/fx and 195 fractions for a total dose of 3997.5 cGy and follow the same procedure except for duplicating the arcs for a total of 13 and recalculating with fixed MUs for a prescription of 4000 cGy in 15 fractions. This yields a plan where each arc is delivering a pulse of 20.5 cGy. Where it is not possible to enter fractional values of centigray, normalization of the final plan should achieve appropriate dosing.

3.1.2. 3D-DCA with two half arcs

For conventional fractionation, create a plan with 40 cGy/fx and 115 fractions (35 for boost) for a total dose of 4600 cGy (1400 cGy) using two half arcs with a control point spacing not exceeding 5° (or as above) and a weighting of 50 % each. After dose calculation and normalization, create copies of each arc for a total of ten arcs with the arc direction reversed on alternating arcs and their weights set to 10 %. The plan is then recalculated with fixed MUs for a prescription of 200 cGy/fx as above (Tab. S1). The resulting dose distribution for an example DCA plan is shown in the center column of Figure 1.

For hypofractionation, create a plan with 38 cGy/fx and 105 fractions and follow the same steps except for duplicating the arcs for a total of 14 and recalculating with fixed MUs for a prescription of 4000 cGy in 15 fractions.

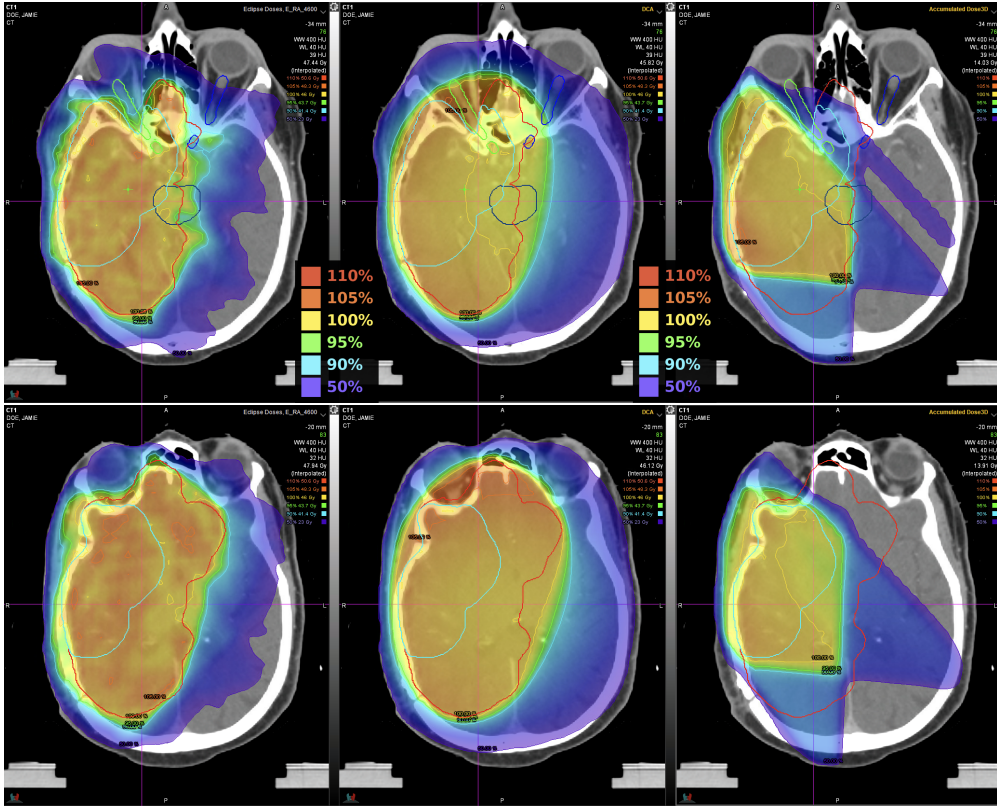


Figure 1: Example dose distributions of single-arc VMAT (left) and DCA (center), and a static 3D-CRT (right) plans to 4600 cGy, and a static 3D-CRT (right) plan to 1400 cGy. For each two separate axial planes are shown in rows. Structures delineated in red and light blue are PTV4600 and PTV6000, respectively. Colorwash levels are chosen as 110 %, 105 %, 100 %, 95 %, 90 %, and 50 % of the respective prescription doses; yellow corresponds to 100 %.

3.1.3. 3D with static fields and accessories

Create a plan with 200 cGy/fx and 23 fractions (7 for boost) for conventional fractionation and with 267 cGy/fx and 15 fractions for hypofractionation. Place three fields based on target geometry and avoidance of overlapping OARs.

Before manipulating the fields, a pulse distribution for the three fields must be chosen. There are 10 pulses for conventional fractionation and 13 to 14 for hypofractionation. The number of pulses assigned to each field determines its weight to be entered e.g., four pulses in conventional fractionation correspond to a weight of 40 % whereas four out of 14 pulses in hypofrac-

tionation corresponds to a weight of 4/14, or $\approx 28.6\%$. Examples of pulse assignment and corresponding field weights are given in Table 2. After pulse assignment and weighting the fields may be manipulated using accessories like wedges, field-in-field, or electronic compensator. With the latter, care must be taken to keep the relative field weights equal to maintain the same dose delivered in each pulse.

Once an acceptable plan has been generated, each of the fields should be copied according to its pulse assignment. For example, a field with 4/10 pulses will be copied for total of 4 identical fields or a field with 5/14 pulses will be copied for a total of 5

Table 2: Example of pulse assignment for static 3D-CRT with corresponding field weighting. Conventional fractionation uses 10 pulses whereas hypofractionation uses 14 pulses.

#pulses	pulse assignment (weight)		
	Field 1	Field 2	Field 3
10	4 (40 %)	4 (40 %)	2 (20 %)
10	4 (40 %)	3 (30 %)	3 (30 %)
10	5 (50 %)	3 (30 %)	2 (20 %)
13	5 (38 %)	5 (38 %)	3 (24 %)
13	5 (38 %)	4 (31 %)	4 (31 %)
14	5 (35.7 %)	5 (35.7 %)	4 (28.6 %)
14	6 (42.8 %)	4 (28.6 %)	4 (28.6 %)
14	6 (42.8 %)	5 (35.7 %)	3 (21.5 %)

identical fields (Tab. S1). The field weights should then be normalized to sum to 100 %. For conventional fractionation this means that each field will have a weight of 10 %. The resulting dose distribution for an example static 3D-CRT boost plan is shown in the right column of Figure 1.

3.2. Plan evaluation metrics

Plans were created for conventional fractionation including the initial and boost plans. VMAT was used on three different units whereas for 3D-CRT only one set of plans was created using DCA for the initial and static fields for the boost plan.

Most plans complied with ideal constraints and achieved similar heterogeneity and conformity metrics tabulated in Table 3. Where they did not acceptable variations were met for $D_{10\%}$ and $D_{0.03\text{cm}^3}$. In order to comply with dose constraints for brainstem, optic chiasm and nerves, the 3D-CRT boost plan did not achieve full coverage as indicated by the low CI_{TV} ; it did, however, achieve the protocol's variation acceptable for $D_{95\%}$. Homogeneities in VMAT plans treating the 4600 cGy and

6000 cGy volumes were ≤ 0.8 and ≤ 0.13 , respectively. In these plans $CI_{Paddick}$ were ≥ 0.91 and ≥ 0.84 with differences driven by variations in CI_{PIV} .

3.3. Plan delivery measurements

Ionization chamber measurements for each pulse of the plans described above are given in Table 4. Deviations from the expected mean dose at the chamber area were within 1.4 % for all plans and pulses. Measurement variations over at least five replicates per configuration were 1 % or less.

The average fractions of points in the EPID measurements with $\Gamma(1\%, 1\text{mm}) < 1$ were 91.0(1) %, 97.2(2) %, and 88.9(16) % for the TrueBeam Edge, Halcyon, and Trilogy units, respectively. Only points above a 10 % dose threshold were included in the analysis and dose distributions were normalized to maximum dose. When increasing to a clinically more commonly used dose difference threshold of 2 %, these increased to 96.2(3) %, 99.2 %, and 96.8(8) %. On the Trilogy unit, the plan created with the highest set dose rate available had 28.3(40) % and 94.3(10) % of points with $\Gamma < 1$ for dose difference thresholds of 1 % and 5 %, respectively.

4. Discussion

4.1. Planning recipes

Several beam geometries were initially considered for VMAT, specifically two arcs with complementary collimator angles in addition to the single arc setup discussed here. Using complementary collimator angles results in substantially increased degrees of freedom for the optimization, e.g., $N_{\text{dof}}(0, 90^\circ) \sim N_{\text{dof}}(0) \times N_{\text{dof}}(90^\circ)$ compared to $N_{\text{dof}}(0, 0) \sim 2 N_{\text{dof}}(0)$. This is typically desirable to simultaneously improve target

Table 3: Evaluation metrics for conventional fractionation plans generated per the recipes. Absorbed doses are given in percent of prescription unless explicitly specified. For 3D-CRT, DCA was used for the initial plan and static fields were used for the boost plan. Differences between the stated values for CI and its factors are due to rounding.

*met variation acceptable only

D_{Rx}	Plan (unit)	$D_{95.0\%}$	$D_{10.0\%}$	$D_{0.03\text{ cm}^3}$	HI	$CI_{Paddick}$	CI_{TV}	CI_{PIV}
4600 cGy	VMAT (Edge)	100.1	103.9	107.1*	0.06	0.92	0.95	0.96
4600 cGy	VMAT (Halcyon)	100.0	105.4*	109.5*	0.08	0.91	0.95	0.96
4600 cGy	VMAT (Trilogy)	100.0	104.5	107.9*	0.07	0.91	0.95	0.96
6000 cGy	VMAT (Edge)	99.1	103.8	106.4	0.11	0.86	0.94	0.92
6000 cGy	VMAT (Halcyon)	100.0	106.4*	109.4*	0.13	0.84	0.95	0.88
6000 cGy	VMAT (Trilogy)	99.8	105.1*	108.3*	0.12	0.84	0.95	0.88
4600 cGy	3D-DCA (Edge)	98.8	105.4*	110.0*	0.10	0.75	0.87	0.86
6000 cGy	3D (Edge)	95.7*	100.0	101.9	0.13	0.06	0.10	0.59

Table 4: In-phantom ionization chamber measurements in high dose and low gradient regions of individual fields (pulses) of each plan delivered on a TrueBeam Edge unit. Where no uncertainty is given it was less than the significant digit.

Field	D_{meas} / cGy	D_{TPS} / cGy	Δ_{rel} / %
<i>VMAT single arc</i>			
CW	21.2(1)	20.9(2)	1.4
CCW	21.1(1)	20.9(2)	0.9
<i>3D-DCA with two half arcs</i>			
Arc 1	18.0	17.9(1)	0.6
Arc 2	23.2	23.0(1)	0.9
<i>3D static with accessories</i>			
A1	24.0	23.7(2)	1.3
A2	20.3	20.4(2)	-0.5
A3	18.7	18.6(2)	0.5

dose conformality and homogeneity, and critical OAR avoidance. We found, however, that this can lead to substantial differences in field doses of each arc as shown in Figures 2 and S1. Furthermore, it is commonly not possible to apply optimization constraints on homogeneity to individual fields (as this would also run counter

to improving the N_{dof}), nor is a per-field dose evaluation commonly performed in the TPS. This poses an issue for TMPRT where each pulse is supposed to deliver a portion of the fraction dose, around 15 cGy to 25 cGy, to exploit radiation hypersensitivity. Reviewing the anatomy of several GBM cases informed the recommendation to use collimator angles that result in the MLC leaves moving along the superior-inferior direction i.e., around 90° (IEC scale).

Splitting the DCA delivery into two half arcs was required due to machine limitations on all considered units, specifically the lower limit for delivered monitor units per degree. On the more modern TrueBeam Edge and Halcyon systems this limit is 0.1 MU/°, while for older units like the Trilogy it may be higher (0.3 MU/°). Other manufacturers' LINACs may have similar limitations, which must be considered individually when commissioning TMPRT. While this limit also applies to VMAT arcs they typically require more than 36 MU to accommodate modulation. In contrast to the two-arc VMAT solution, however, us-

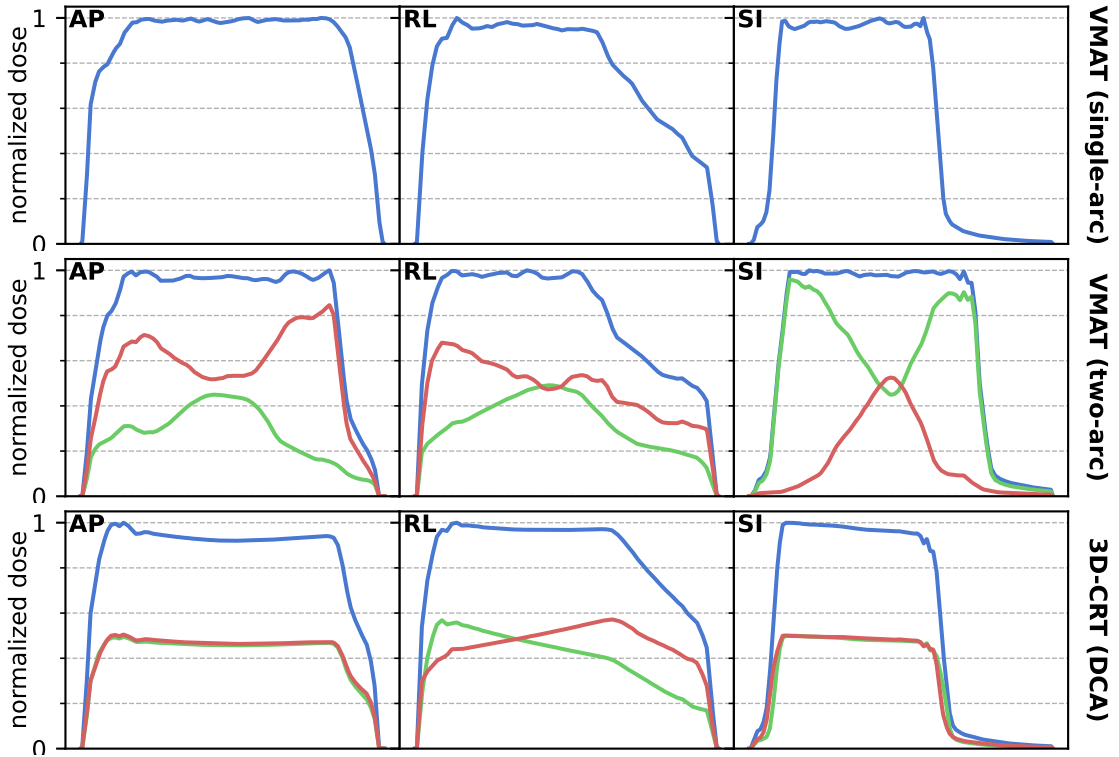


Figure 2: Dose profiles for single- and two-arc VMAT (top and middle) and DCA (bottom) showing the plan total (blue) and field (red, green) dose profiles in three directions through isocenter. Note that any profile alignment across different plans are coincidental. AP: anterior-posterior; RL: right-left; SI: superior-inferior.

ing two DCAs did not yield substantially different field doses as shown in Figures 2 and S2. Profiles along the anterior-posterior and superior-inferior directions were almost identical. Only in the left-right direction a gradient was observed across the field, which is expected since the delivery consists of partial arcs covering the left and right hemispheres. A similar behavior was observed for the static 3D-CRT plan with field doses and profiles shown in Figure S3.

VMAT using a single arc presents the overall best treatment planning and delivery technique for TMPRT due to its flexibility in achieving conformal and homogeneous dose distributions and simultaneous OAR sparing. 3D-CRT techniques can provide an acceptable fallback solution where insur-

ance or technical limitations (no VMAT capability) exist. While helical tomotherapy delivery is excluded in the proposed trial, users of those units may refer to a previous publication for off-trial treatments.^{27,28}

4.2. Achieved plan metrics

Despite the constraints of using only one VMAT arc high plan quality was achieved for the three diverse LINACs, each using a different MLC model. There was no clear trend of either units yielding better plan metrics (Tab. 3).

For 3D-CRT a combination of DCA and static fields with dynamic wedges and sub-fields was chosen primarily to demonstrate both planning techniques. The utility of DCA strongly depends on the target shape

but requires less planning effort to generate a mostly uniform dose distribution compared to static fields. On the other hand, sparing of critical OARs like optic structures and the brainstem, which are often adjacent or encompassed in the target margins is often more easily accomplished using static fields with MLC manipulation.

While the recommendations presented are based on a single patient's geometry, we reviewed several patients to select the most challenging target geometry with respect to total volume, shape, and overlap with critical OARs. In any case, it will be important to consider each patient's individual anatomy in the planning process.

4.3. Plan delivery measurements

Agreement between measured point doses and TPS values in high dose, low gradient areas showed that treatment delivery at low dose rates of 100 MU/min (or lower during VMAT) is consistent and per plan. Differences for VMAT delivery were higher than for DCA but not larger than 1.4 %, highlighting that MLC position uncertainty, dose rate and gantry speed variations are likely to have negligible impact. Uncertainties in the position and attenuation properties of the used support structures could contribute to the observed differences, which is corroborated by the larger variation being observed for the posterior wedged field (A1) in static 3D-CRT.

Portal dosimetry modes on the more modern TrueBeam and Halcyon units use a single calibration factor across all dose rates. This is possible since their EPID response does not vary substantially across the typical range of dose rates in conventional RT. This is supported by the high Γ -pass rates for VMAT plans with

average dose rates of \approx 100 MU/min compared to the typical calibration dose rate of 400 MU/min to 600 MU/min. In contrast, on older units like the Trilogy EPID dosimetry modes uses individual calibration factors for each possible set dose rate due to an increased dose rate dependence. While the choice of set dose rate does not affect plan optimization or delivery, it affects EPID dosimetry accuracy. This was demonstrated by the large difference between Γ -pass rates for 600 MU/min (28 %) and 100 MU/min (94 %) set dose rates, where in both cases the machine delivered dose rate was fluctuating around 100 MU/min. It is thus recommended to choose the set dose rate closest to the expected average.

5. Conclusions

Treatment planning for TMPRT was shown to be feasible with single-arc VMAT and 3D-CRT. VMAT is preferred to achieve optimal homogeneity, conformality, and OAR sparing. Measurement-based plan verification of low-dose rate field/pulse delivery showed that both modern and legacy LINACs are capable to deliver TMPRT plans with high fidelity.

References

- [1] D. Brenner, E. Hall, Conditions for the equivalence of continuous to pulsed low dose rate brachytherapy, *International Journal of Radiation Oncology*Biology*Physics* 20 (1) (1991) 181–190. [doi:10.1016/0360-3016\(91\)90158-z](https://doi.org/10.1016/0360-3016(91)90158-z).
- [2] B. Pierquin, Curie medal lecture 2000 The optimization of delivered dose in radiotherapy: is it related to low dose rate?, *Radiotherapy and Oncology* 58 (1) (2001) 7–9. [doi:10.1016/s0167-8140\(00\)00271-1](https://doi.org/10.1016/s0167-8140(00)00271-1).

- [3] C. T. Schultz, C. R. Geard, Radioresponse of human astrocytic tumors across grade as a function of acute and chronic irradiation, International Journal of Radiation Oncology*Biology*Physics 19 (6) (1990) 1397–1403. [doi:10.1016/0360-3016\(90\)90350-s](https://doi.org/10.1016/0360-3016(90)90350-s).
- [4] C. J. Schultz, D. K. Gaffney, M. J. Lindstrom, T. J. Kinsella, Iododeoxyuridine radiosensitization of human glioblastoma cells exposed to acute and chronic gamma irradiation: mechanistic implications and clinical relevance., The cancer journal from Scientific American 1 (2) (1995) 151–61.
- [5] M. C. Joiner, B. Marples, P. Lambin, S. C. Short, I. Turesson, Low-dose hypersensitivity: current status and possible mechanisms, International Journal of Radiation Oncology*Biology*Physics 49 (2) (2001) 379–389. [doi:10.1016/s0360-3016\(00\)01471-1](https://doi.org/10.1016/s0360-3016(00)01471-1).
- [6] S. C. Short, J. Kelly, C. R. Mayes, M. Woodcock, M. C. Joiner, Low-dose hypersensitivity after fractionated low-dose irradiation in vitro, International Journal of Radiation Biology 77 (6) (2001) 655–664. [doi:10.1080/09553000110041326](https://doi.org/10.1080/09553000110041326).
- [7] S. A. Krueger, M. C. Joiner, M. Weinfeld, E. Piasentin, B. Marples, Role of Apoptosis in Low-Dose Hyper-radiosensitivity, Radiation Research 167 (3) (2007) 260–267. [doi:10.1667/rr0776.1](https://doi.org/10.1667/rr0776.1).
- [8] B. Marples, S. J. Collis, Low-Dose Hyper-Radiosensitivity: Past, Present, and Future, International Journal of Radiation Oncology*Biology*Physics 70 (5) (2008) 1310–1318. [doi:10.1016/j.ijrobp.2007.11.071](https://doi.org/10.1016/j.ijrobp.2007.11.071).
- [9] W. A. Tomé, S. P. Howard, On the possible increase in local tumour control probability for gliomas exhibiting low dose hyper-radiosensitivity using a pulsed schedule, The British Journal of Radiology 80 (949) (2007) 32–37. [doi:10.1259/bjr/15764945](https://doi.org/10.1259/bjr/15764945).
- [10] J. T. Dilworth, S. A. Krueger, M. Dabjan, I. S. Grills, J. Torma, G. D. Wilson, B. Marples, Pulsed low-dose irradiation of orthotopic glioblastoma multiforme (GBM) in a pre-clinical model: Effects on vascularization and tumor control, Radiotherapy and Oncology 108 (1) (2013) 149–154. [doi:10.1016/j.radonc.2013.05.022](https://doi.org/10.1016/j.radonc.2013.05.022).
- [11] D. Y. Lee, J. L. Chunta, S. S. Park, J. Huang, A. A. Martinez, I. S. Grills, S. A. Krueger, G. D. Wilson, B. Marples, Pulsed Versus Conventional Radiation Therapy in Combination With Temozolomide in a Murine Orthotopic Model of Glioblastoma Multiforme, International Journal of Radiation Oncology*Biology*Physics 86 (5) (2013) 978–985. [doi:10.1016/j.ijrobp.2013.04.034](https://doi.org/10.1016/j.ijrobp.2013.04.034).
- [12] K. Meyer, S. A. Krueger, J. L. Kane, T. G. Wilson, A. Hanna, M. Dabjan, K. M. Hege, G. D. Wilson, I. Grills, B. Marples, Pulsed Radiation Therapy With Concurrent Cisplatin Results in Superior Tumor Growth Delay in a Head and Neck Squamous Cell Carcinoma Murine Model, International Journal of Radiation Oncology*Biology*Physics 96 (1) (2016) 161–169. [doi:10.1016/j.ijrobp.2016.04.031](https://doi.org/10.1016/j.ijrobp.2016.04.031).
- [13] J. B. Adkison, W. Tomé, S. Seo, G. M. Richards, H. I. Robins, K. Rasmussen, J. S. Welsh, P. A. Mahler, S. P. Howard, Reirradiation of Large-Volume Recurrent Glioma With Pulsed Reduced-Dose-Rate Radiotherapy, International Journal of Radiation Oncology*Biology*Physics 79 (3) (2011) 835–841. [doi:10.1016/j.ijrobp.2009.11.058](https://doi.org/10.1016/j.ijrobp.2009.11.058).
- [14] J. A. Bovi, M. A. Prah, A. A. Retzlaff, K. M. Schmailinda, J. M. Connelly, S. D. Rand, C. S. Marszalkowski, W. M. Mueller, M. L. Siker, C. J. Schultz, Pulsed Reduced Dose Rate Radiotherapy in Conjunction With Bevacizumab or Bevacizumab Alone in Recurrent High-grade Glioma: Survival Outcomes, International Journal of Radiation Oncology*Biology*Physics 108 (4) (2020) 979–986. [doi:10.1016/j.ijrobp.2020.06.020](https://doi.org/10.1016/j.ijrobp.2020.06.020).
- [15] A. R. Burr, H. I. Robins, R. A. Bayliss, S. P. Howard, Pulsed Reduced Dose Rate for Reirradiation of Recurrent Breast Cancer, Practical Radiation Oncology 10 (2) (2020) e61–e70. [doi:10.1016/j.prro.2019.09.004](https://doi.org/10.1016/j.prro.2019.09.004).
- [16] A. R. Burr, H. I. Robins, R. A. Bayliss, A. M. Baschnagel, J. S. Welsh, W. A. Tomé, S. P.

- Howard, Outcomes From Whole-Brain Reirradiation Using Pulsed Reduced Dose Rate Radiation Therapy, *Advances in Radiation Oncology* 5 (5) (2020) 834–839. [doi:10.1016/j.adro.2020.06.021](https://doi.org/10.1016/j.adro.2020.06.021).
- [17] C. T. Lee, Y. Dong, T. Li, S. Freedman, J. Anaokar, T. J. Galloway, M. A. Hallman, S. E. Weiss, S. B. Hayes, R. A. Price, C. C. Ma, J. E. Meyer, Local Control and Toxicity of External Beam Reirradiation With a Pulsed Low-dose-rate Technique, *International Journal of Radiation Oncology*Biology*Physics* 100 (4) (2018) 959–964. [doi:10.1016/j.ijrobp.2017.12.012](https://doi.org/10.1016/j.ijrobp.2017.12.012).
- [18] P. Mohindra, H. I. Robins, W. A. Tomé, L. Hayes, S. P. Howard, Wide-field pulsed reduced dose rate radiotherapy (PRDR) for recurrent ependymoma in pediatric and young adult patients., *Anticancer research* 33 (6) (2013) 2611–8.
- [19] E. S. Murphy, K. Rogacki, A. Godley, P. Qi, C. A. Reddy, M. S. Ahluwalia, D. M. Peereboom, G. H. Stevens, J. S. Yu, R. Kotecha, J. H. Suh, S. T. Chao, Intensity modulated radiation therapy with pulsed reduced dose rate as a reirradiation strategy for recurrent central nervous system tumors: An institutional series and literature review, *Practical Radiation Oncology* 7 (6) (2017) e391–e399. [doi:10.1016/j.prro.2017.04.003](https://doi.org/10.1016/j.prro.2017.04.003).
- [20] G. M. Richards, W. A. Tomé, H. I. Robins, J. A. Stewart, J. S. Welsh, P. A. Mahler, S. P. Howard, Pulsed reduced dose-rate radiotherapy: a novel locoregional retreatment strategy for breast cancer recurrence in the previously irradiated chest wall, axilla, or supraclavicular region, *Breast Cancer Research and Treatment* 114 (2) (2009) 307–313. [doi:10.1007/s10549-008-9995-3](https://doi.org/10.1007/s10549-008-9995-3).
- [21] J. S. Witt, H. B. Musunuru, R. A. Bayliss, S. P. Howard, Large volume re-irradiation for recurrent meningioma with pulsed reduced dose rate radiotherapy, *Journal of Neuro-Oncology* 141 (1) (2019) 103–109. [doi:10.1007/s11060-018-03011-z](https://doi.org/10.1007/s11060-018-03011-z).
- [22] J. Yan, J. Yang, Y. Yang, W. Ren, J. Liu, S. Gao, S. Li, W. Kong, L. Zhu, M. Yang, X. Qian, B. Liu, Use of Pulsed Low-Dose Rate Radiotherapy in Refractory Malignancies, *Translational Oncology* 11 (1) (2018) 175–181. [doi:10.1016/j.tranon.2017.12.004](https://doi.org/10.1016/j.tranon.2017.12.004).
- [23] M. F. Almahariq, T. J. Quinn, J. D. Arden, P. T. Roskos, G. D. Wilson, B. Marples, I. S. Grills, P. Y. Chen, D. J. Krauss, P. Chin-naiyan, J. T. Dilworth, Pulsed radiation therapy for the treatment of newly diagnosed glioblastoma, *Neuro-Oncology* 23 (3) (2020) 447–456. [doi:10.1093/neuonc/noaa165](https://doi.org/10.1093/neuonc/noaa165).
- [24] D. N. Yeboa, S. E. Braunstein, A. Cabrera, K. Crago, E. Galanis, E. M. Hattab, D. E. Heron, J. Huang, M. M. Kim, J. P. Kirkpatrick, J. P. Knisely, M. F. McAleer, S. McClelland, M. T. Milano, J. Moliterno, A. Porter, K. J. Redmond, D. M. Trifiletti, C. Tsien, B. P. Venkatesulu, Y. Vinogradskiy, L. Bradfield, A. R. Helms, J. A. Bovi, Radiation Therapy for WHO Grade 4 Adult-Type Diffuse Glioma: An ASTRO Clinical Practice Guideline, *Practical Radiation Oncology* 15 (5) (2025) 451–471. [doi:10.1016/j.prro.2025.05.014](https://doi.org/10.1016/j.prro.2025.05.014).
- [25] International Commission on Radiation Units and Measurements, ICRU Report 83: Prescribing, recording, and reporting photon-beam intensity-modulated radiation therapy (IMRT) (2010).
- [26] I. Paddick, [A simple scoring ratio to index the conformity of radiosurgical treatment plans: Technical note](#), *Journal of Neurosurgery* 93 (supplement_3) (2000) 219–222. [doi:10.3171/jns.2000.93.supplement_3.0219](https://doi.org/10.3171/jns.2000.93.supplement_3.0219). URL https://thejns.org/view/journals/j-neurosurg/93/supplement_3/article-p219.xml
- [27] K. H. Rasmussen, N. Hardcastle, S. P. Howard, W. A. Tomé, Reirradiation of Glioblastoma through the Use of a Reduced Dose Rate on a Tomotherapy Unit, *Technology in Cancer Research & Treatment* 9 (4) (2010) 399–406. [doi:10.1177/153303461000900409](https://doi.org/10.1177/153303461000900409).
- [28] Y. Rong, B. Paliwal, S. P. Howard, J. Welsh, Treatment Planning for Pulsed Reduced Dose-Rate Radiotherapy in Helical Tomotherapy,

International Journal of Radiation Oncology*Biology*Physics 79 (3) (2011) 934–942.
[doi:10.1016/j.ijrobp.2010.05.055](https://doi.org/10.1016/j.ijrobp.2010.05.055).

Appendix

Table 5: Absolute dose target and OAR constraints given in centigray as proposed by the NRG-CC017 trial.

*conventional fractionation; #hypofractionation

Volume	Metric	Unit	<i>conventional fractionation</i>		<i>hypofractionation</i>	
			Constraint	Accept. Var.	Constraint	Accept. Var.
PTV4600*	$D_{95\%}$	cGy	≥ 4600	≥ 4370	n/a	n/a
PTV6000*	$D_{95\%}$	cGy	≥ 5925	≥ 5700	n/a	n/a
	$D_{10\%}$	cGy	≤ 6300	≤ 6500	n/a	n/a
	$D_{0.03\text{ cm}^3}$	cGy	≤ 6400	≤ 6600	n/a	n/a
PTV4000#	$D_{95\%}$	cGy	n/a	n/a	≥ 3955	≥ 3800
	$D_{10\%}$	cGy	n/a	n/a	≤ 4200	≤ 4340
	$D_{0.03\text{ cm}^3}$	cGy	n/a	n/a	≤ 4270	≤ 4400
Brainstem	$D_{0.03\text{ cm}^3}$	cGy	≤ 5500	≤ 6000	≤ 4500	≤ 4800
Optic structures (PRV)	$D_{0.03\text{ cm}^3}$	cGy	≤ 5500	≤ 6000	≤ 4000	≤ 4200
Retinas (lt/rt)	$D_{0.03\text{ cm}^3}$	cGy	≤ 4500	≤ 5000	≤ 3500	≤ 3750
Lenses (lt/rt)	$D_{0.03\text{ cm}^3}$	cGy	≤ 1000	ALARA	≤ 900	ALARA
Spinal cord	$D_{0.03\text{ cm}^3}$	cGy	≤ 5000	none	≤ 4200	none

Supplementary Material

Table S1: Beam parameter list for the example static and DCA 3D-CRT, and (single-arc) VMAT plans created following the planning recipes.

Id	MLC	Weight	Gantry	Coll.	Wedge	X1	X2	Y1	Y2	MU
<i>static 3D-CRT</i>										
A1 1	Static	0.100	180.0E	90.0	EDW30IN	3.3	3.7	4.5	3.3	30
A1 2	Static	0.100	180.0E	90.0	EDW30IN	3.3	3.7	4.5	3.3	30
A1 3	Static	0.100	180.0E	90.0	EDW30IN	3.3	3.7	4.5	3.3	30
A2 1	Static	0.100	320.0	345.0	None	5.4	4.6	4.0	3.6	23
A2 2	Static	0.100	320.0	345.0	None	5.4	4.6	4.0	3.6	23
A2 3	Static	0.100	320.0	345.0	None	5.4	4.6	4.0	3.6	23
A2 4	Static	0.100	320.0	345.0	None	5.4	4.6	4.0	3.6	23
A3 1	Static	0.100	100.0	90.0	EDW25IN	3.3	3.6	5.1	5.7	27
A3 2	Static	0.100	100.0	90.0	EDW25IN	3.3	3.6	5.1	5.7	27
A3 3	Static	0.100	100.0	90.0	EDW25IN	3.3	3.6	5.1	5.7	27
<i>dynamic conformal arc (DCA)</i>										
A1 CW	Arc Dynamic	0.100	181.0 CW 0.0	10.0						23
A2 CW	Arc Dynamic	0.100	0.0 CW 179.0	10.0						26
A3 CCW	Arc Dynamic	0.100	179.0 CCW 0.0	10.0						26
A4 CCW	Arc Dynamic	0.100	0.0 CCW 181.0	10.0						23
A5 CW	Arc Dynamic	0.100	181.0 CW 0.0	10.0						23
A6 CW	Arc Dynamic	0.100	0.0 CW 179.0	10.0						26
A7 CCW	Arc Dynamic	0.100	179.0 CCW 0.0	10.0						26
A8 CCW	Arc Dynamic	0.100	0.0 CCW 181.0	10.0						23
A9 CW	Arc Dynamic	0.100	181.0 CW 0.0	10.0						23
A10 CW	Arc Dynamic	0.100	0.0 CW 179.0	10.0						26
<i>volumetric modulated arc therapy (VMAT)</i>										
A1	VMAT	0.453	181.0 CW 179.0	70.0						91
A2	VMAT	0.453	179.0 CCW 181.0	70.0						91
A3	VMAT	0.453	181.0 CW 179.0	70.0						91
A4	VMAT	0.453	179.0 CCW 181.0	70.0						91
A5	VMAT	0.453	181.0 CW 179.0	70.0						91
A6	VMAT	0.453	179.0 CCW 181.0	70.0						91
A7	VMAT	0.453	181.0 CW 179.0	70.0						91
A8	VMAT	0.453	179.0 CCW 181.0	70.0						91
A9	VMAT	0.453	181.0 CW 179.0	70.0						91
A10	VMAT	0.453	179.0 CCW 181.0	70.0						91

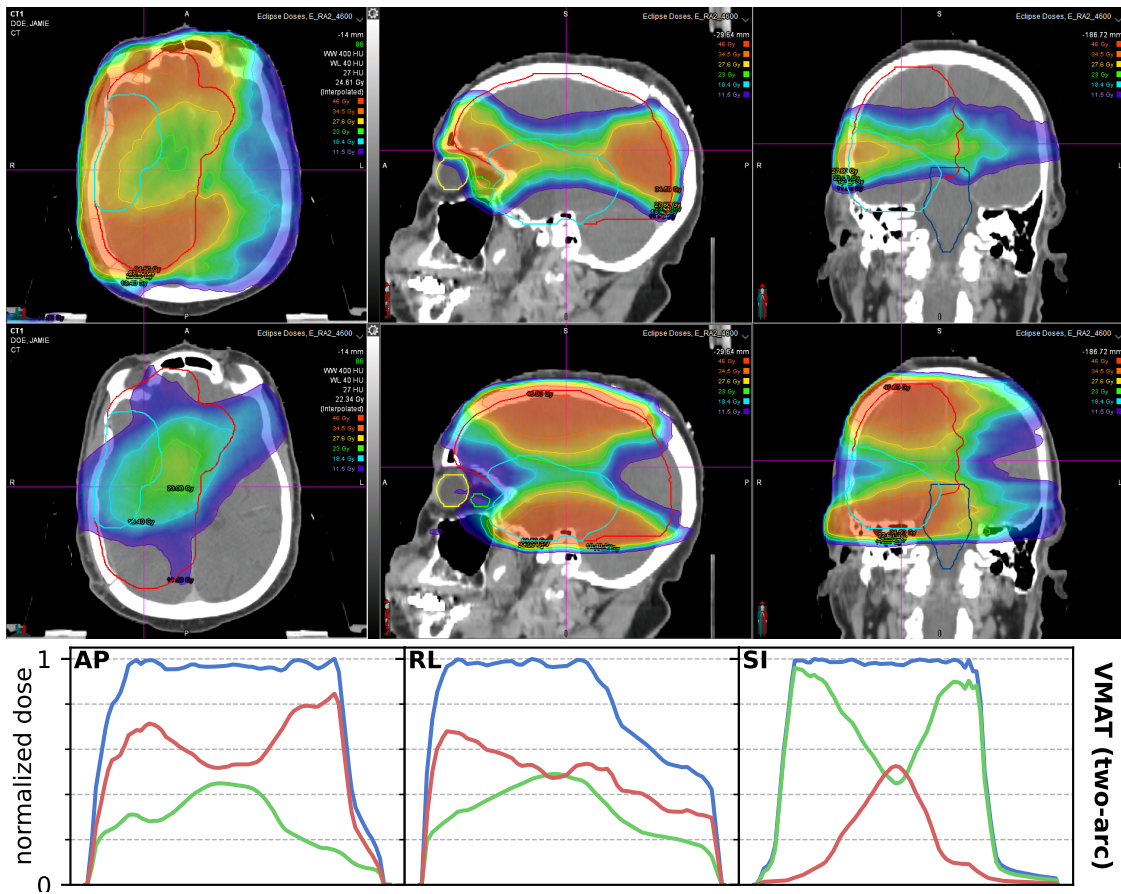


Figure S1: Field doses and profiles for an example two-arc VMAT plan. Arcs one and two are shown in the top and bottom row with HIs of 1.47 and 1.60, respectively. To deliver 4600 cGy total, each arc is supposed to contribute 2300 cGy; levels in the colorwash are chosen as 200 %, 150 %, 120 %, 100 %, 80 %, and 50 % of 2300 cGy.

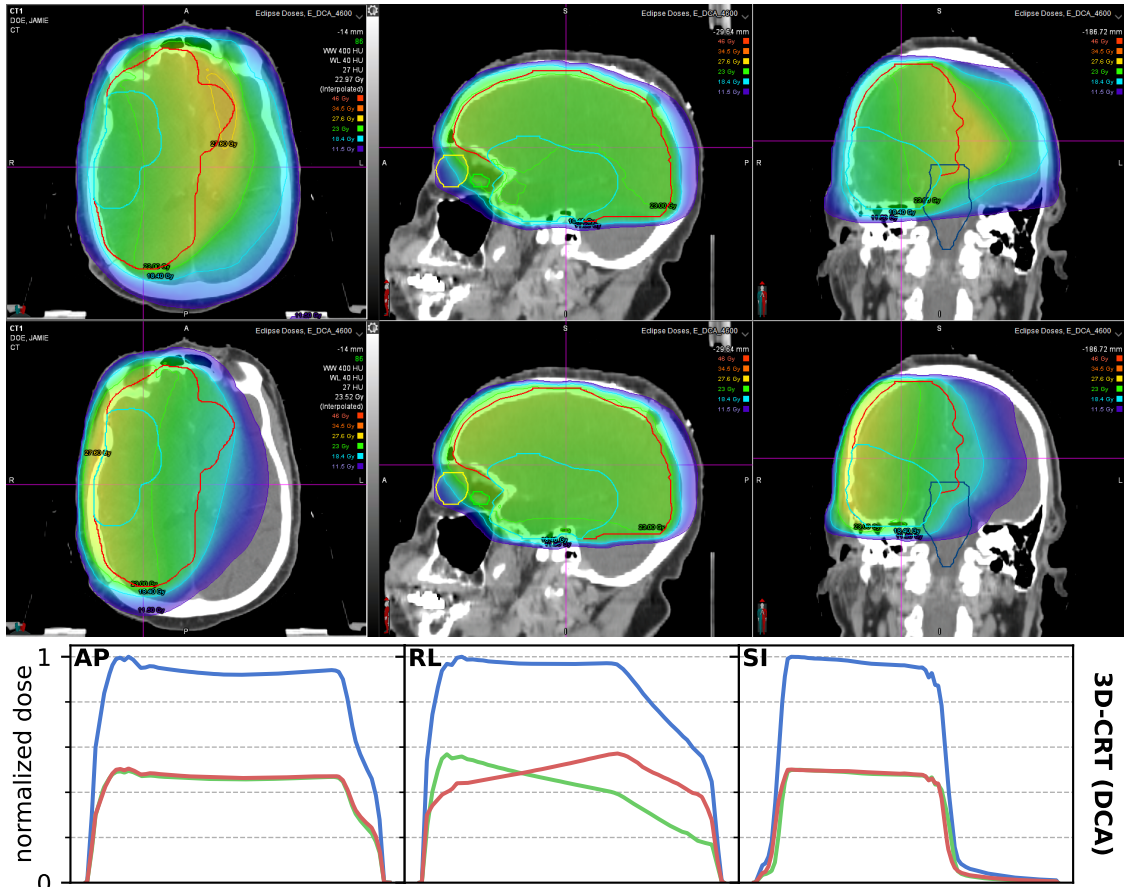


Figure S2: Field doses and profiles for an example two-arc DCA plan. Arcs one and two are shown in the top and bottom row with HIs of 0.28 and 0.27, respectively. To deliver 4600 cGy total, each arc is supposed to contribute 2300 cGy; levels in the colorwash are chosen as 200 %, 150 %, 120 %, 100 %, 80 %, and 50 % of 2300 cGy.

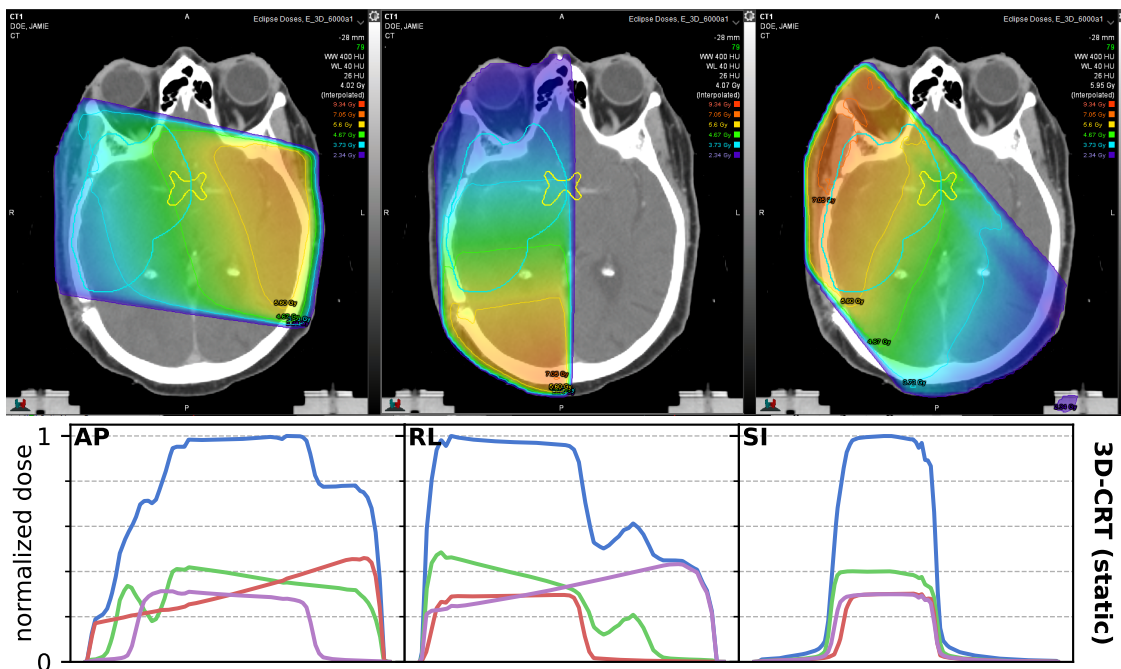


Figure S3: Field doses and profiles through isocenter for an example three-field 3D-CRT boost plan using wedges and MLC with HIs of 0.38, 0.52, and 0.44. Levels in the colorwash are chosen as 200 %, 150 %, 120 %, 100 %, 80 %, and 50 % of 467 cGy.